International Journal of Advanced Technology and Engineering Exploration, Vol 11(110)
ISSN (Print): 2394-5443 ISSN (Online): 2394-7454
http://dx.doi.org/10.19101/IJATEE.2022.10100447

Research Article

Enhancing infrastructure sustainability: reliability and sensitivity analysis of localized integrated renewable energy systems using feed forward backpropagation neural network

Nitin Kumar Sharma[1*], Sachin Kumar[2], Pradeep Kumar Yadav[3] and Ekata[2]
Assistant Professor, Department of Applied Sciences and Humanities, Ajay Kumar Garg Engineering College, Ghaziabad, UP, 201009, India[1]
Professor, Department of Applied Sciences, Krishna Institute of Engineering and Technology, Delhi-NCR, Ghaziabad, Uttar Pradesh, 201206, India[2]
Principle Technical Officer, Central Building Research Institute, Roorkee, Uttarakhand, 247667, India[3]

Received: 20-November-2022; Revised: 20-December-2023; Accepted: 23-December-2023

Abstract
Establishing robust infrastructure and securing a sustainable power supply can be costly and time-consuming. Localized power generation from natural resources through integrated renewable energy systems (IRESs) offers a solution. This study explores the reliability and key statistics of an IRES incorporating solar photovoltaic modules, wind turbines, and battery banks. The failure and repair rates follow an exponential distribution due to the increased risk in integrated structures. Neural networks (NN), particularly the feed forward back propagation neural network (FFBPNN), enhance the consistency and precision of reliability parameters. The learning process of FFBPNN adjusts neural weights, improving parameter values. Utilizing the MATLAB algorithm, this study iterated until achieving accuracy close to 0.0001. The proposed system's real-time operations can be effectively managed by analyzing operational costs and system sensitivity to different parameters.

Keywords
Neural architecture, Battery bank, Reliability, Non-conventional energy sources, Photovoltaic.

1.Introduction
Energy can be found in various forms in nature. Electricity has a significant place among the numerous forms of energy. It is necessary to discover an ideal infrastructure for certain pre-determined objectives by utilizing some appropriate setups. In other words, diluted energy must converge in the direction of some goal. However, it must be ensured that the exhaustion of energy from nature must not be destructive to the ecosystem since it is evidenced that humans have obliterated nature's self-balancing capacity in many areas in the drive for technology and other advancements [1]. Energy resources can be subdivided into two broad categories based on their potential availability: conventional and non-conventional energy sources. Conventional energy sources are non-renewable energy sources.

Conventional energy-generating systems burn fossil fuels or use hydropower. Non-renewable energy systems rely on a single source for electric power generation, such as coal, gas, hydropower, and nuclear power. The consumption of conventional energy sources by the surging population and industrial sector is depleting and exhausting them at a swift pace. Energy derived from these sources pollutes the environment severely. It has resulted in disasters in some scenarios.

Non-conventional energy sources are renewable energy sources. The systems relying on these sources are known as renewable energy systems since they are revived by nature. These systems can produce electricity from a single source or numerous sources. The backup and storage systems play crucial roles in managing the energy fluctuations of hybrid power plants based on integrated renewable energy systems (IRESs) [2].

*Author for correspondence

Noticeably, urban and rural population uses mini or small solar photovoltaic (PV) battery with grid-connected (on-grid) power systems to reduce monthly electric bills [3]. However, continuous electric power supply in deep rural and isolated locations that are not grid-connected (off-grid) is favored by IRES [3–7]. Non-conventional energy sources, like sunlight, wind, and water, are plentiful. Additionally, they are freely available in some ways from countless natural cycles. These energy sources do not pollute the environment and do not require expensive long-term maintenance due to their inherent natural properties. Therefore, the trend of green energy, which does not damage the environment or natural organisms, must be followed. Studies have reported that efforts are being made for zero carbon emissions during power generation [8].

Jurasz et al. [9] reported that small-scale hybrid power systems based on fluctuating renewable energy sources, like wind and solar, are becoming more and more common since they affect the environment less negatively, use less energy, and deliver more reliable electricity. The reliability of hybrid systems is influenced by the complementary nature of the sources. The increased complementarity improves the system's ability to carry the load (L). Battery bank (BB) or other forms of energy storage can be added to improve the system's reliability. However, the effect of complementarity on reliability declines as the storage capacity increases [9, 10].

This study emphasized on a small standalone IRES that is useful for rural and semi-urban areas facing power fluctuations and cost issues. PV-battery grid-connected modules are popular and commonly used in households and industries [3]. Although they may provide a seamless power supply, they have high initial establishment cost and maintenance. The additional load on the grid increases during the charging of batteries. Sometimes failures occur due to irregular voltage and high charging speed because they decrease the life of batteries. It is more difficult to regulate and supply electric power continuously in rural and remote areas because transmission lines are unable to bear the load of modern lifestyle appliances and have poor maintenance [6, 7]. Therefore, dependence on these on-grid systems is risky. The objective of this article was to analyze an independent and reliable system with easy operation, lower failure rate, and less complex configuration. The proposed IRES with PV-BB-wind turbine (WT) worked off-grid with a uniform/controlled charging rate. The high initial costs would be compensated in a few years.

This study highlighted the reliability, cost, and sensitivity of an IRES, which was composed of advanced devices like bifacial/monocrystalline PV module, vertical axis WT (Darrieus, Savonius type), highly durable industrial grade solar compatible batteries, and an intelligent controlling unit for smooth operation. Earlier reported studies used polycrystalline PV and traditional WT, which had poor efficiency [3]. Section 2 of this article reviewed the previously reported studies to provide a basis for this study. For a better explanation, section 3 discussed the system description, necessary initial assumptions/boundaries, development and solution of mathematical model with transition diagram, and flow of algorithms. Section 4 analyzed the results obtained through section 3, which discussed important reliability parameters in detail with data tables and supporting graphics. Section 5 discussed a comparative analysis of components and results derived from mathematical model of IRES, limitations of the system study are also included in this section. Section 6 stated the conclusions drawn from this study and gave suitable recommendations. The future work/scope and applications are also discussed in this section.

2.Literature review

Until now, many studies have been reported on off-grid IRES reliability, maximum yield, design, and size at reasonable investment costs. When we rely on a single source for electric power generation, we experience voltage variations and power supply instability owing to technical faults [11], environmental breakdowns, and the lack of source availability. This fact drove the notion of IRES [12]. *Figures 1* and *2* depict the availabilities of average solar radiation and wind speed. Northern India has a good amount of sunlight and sufficient wind speed for the setup of a small rooftop WT (e.g. Tulip or Helix type).

Pradhan and Karki [13] assessed the probabilistic dependability of an off-grid small hybrid electric system based on PV-wind for electric power supply in Nepal's rural villages [9]. Hydro storage-based IRESs may be better options for isolated zones [14], while IRESs with PV-WT are significant for areas more than 50 kilometers from the electric power supply grid. Negi and Mathew [15] conducted a study hybrid renewable electric power generation systems and focused on sustainability by highlighting several aspects of the IRES mechanism, sizing, system optimization, storage capabilities, and management [16].

Amuta et al. [6] proposed the architecture of a PV-wind-battery system in Zanjan province of Iran to enhance the reliability of power supply to load with real-time data related to renewable source availability [9]. They used the current cost as an objective function to reduce investment, replacement, operation, and maintenance expenses in IRESs. Liu al. [17] demonstrated that the most suitable setup to meet rural power consumption requirements was a standalone hybrid PV-battery backup system. While considering the dependability index (loss of load likelihood), the goal was to reduce the total lifecycle cost (TLCC).The findings showed that the optimal number of PV panels and batteries decreased, but the TLCC and the cost of system components increased with the rise in the reliability index [18].

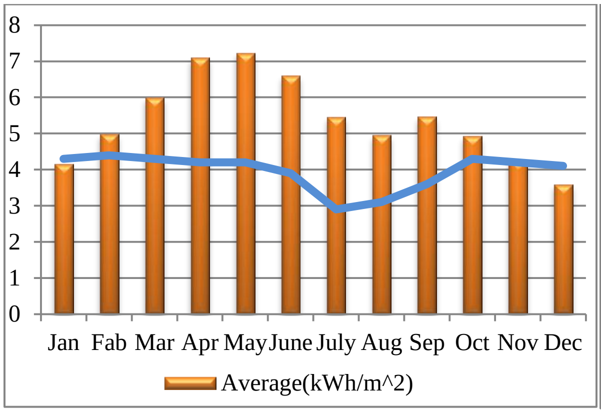

Figure 1 Average solar radiation

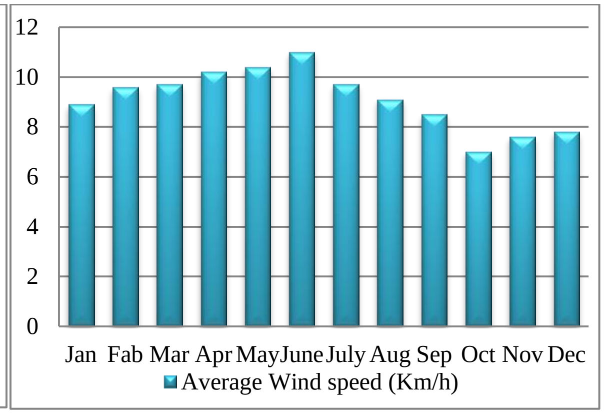

Figure 2 Average windspeed

Reliability is defined as the probability of systems and their components performing their tasks adequately for the intended operating period [19, 13]. Narula et al. [20] investigated the likelihood that South Asian countries would meet 100% of their regional energy demand by 2030 by increasing reliance on power productionbased on IRESs. Patel and Singhal [21] created and verified the IRES model using resources close at hand. Additionally, they asserted that distribution losses and component size impacted the dependability of the system considerably. Sachin and Anand [12] and Ram et al. [22] studied the fundamentals of reliability analysis, reliability improvement techniques of the electrical power distribution system employing electric vehicles (EV) and energy storage systems, and reliability improvement approaches in wind-integrated power systems. They also discussed the dependability effects on reactive power, unit commitment, and protective systems. Another discussion is done on uncertainty in the management of processes involved in the electrical power generation unit then reliability evaluation in distribution systems is well described. An electrical energy power system is efficient if it can supply reasonably continuous and quality electric power to load [23]. Ishani et al. [24] described hybrid renewable energy systems (HRES) for household purposes, which included microprocessors to harness the power of the sun and wind. The project was accomplished according to the available electric powerline. The batteries of the system were charged using solar or wind energy. Microcontrollers were crucial to system control through a maximum power point tracking (MPPT) module or a small alternator. Power sources and loads inside the system were monitored and regulated in real-time. Roy et al. [25] extensively analyzed a hybrid system involving wind and solar-based components from the perspectives of power architectures, mathematical modeling, power electronic converter topologies, and design optimization approaches. They studied numerous hybrid energy storage system coupling techniques, outlining their critical pros and cons. This was done to lower the uncertainty of HRES because including an energy storage system could reduce it even more. Different IRES power converters and cutting-edge control techniques have been studied to examine various combinations of energy sources, modeling, and topologies of power converters, size, and optimization techniques used in hybrid systems [26, 27]. The challenges of technology and IRES-related research were also taken into account. Kallio and Siroux [28] looked at improving solar-based micro-cogeneration systems and micro-cogeneration-based HRES s. In light of the case study's findings, the maximum thermal and electrical reliabilitieswere68% and 70%, respectively. The study suggested that the optimized PV/battery/thermal storage system could not meet the entire energy demand, needing additional sources of heat and power. Jha et al. [29] proposed a dual-energy generating system integrated with a grid to reduce energy waste. The load data was compiled from several areas of Rajasthan, India. The best grid configuration was created using net present cost and cost per unit of energy. Other elements, including inverter optimization, wind energy, and tilt angle optimization for PV arrays, were also used to boost the system's dependability and stability [30]. Sensitivity analysis was carried out to examine the impact of actual fluctuations in capital costs on the established system economy. The simulation results indicated that the average costs of producing power using diesel-based and off-grid systems could be reduced by up to 20% by assuming a 10% annual capacity shortage allowance. According to the cost study, establishing the proposed framework would cost significantly less than other systems. The most popular systems are wind/solar-PV, wind/solar-PV/diesel, and solar-PV/diesel, with and without battery backup, with popularity ratings of 28%, 22%, and 21%, respectively. Remote villages are the most popular among users, followed by islands and communication towers. The average unit prices for wind/solar-PV, wind/solar-PV/diesel, and solar-PV/diesel are about $0.458, $0.355, and $0.349, respectively.

This study rendered a reliability analysis of systems, such as PV modules, WT units, energy storage units, and converters, with the help of various failures/repair parameters using the feed forward back propagation neural network (FFBPNN) of the neural networks (NN) [31, 32]. The reliability of the systems is estimated using many popular methodologies/techniques, such as regenerative point technique, supplementary variable technique [19], stochastic reward nets, and Petri nets. Although these are routine procedures for accurately estimating reliability indicators, the present demand requires improving the output to optimization and reduced error. Hellel et al. [33] used the deterministic and stochastic Petri nets to explore the dynamic behavior in the performance of various renewable energy generating systems (mono or multi-source) in terms of reliability and availability of units.

The integration and combination of renewable energy sources are gaining popularity over time. This study provided an overview of the technologies of HRES, their key problems and design-stage difficulties. The power generation technology choices and unit sizing, system layouts, and energy management and control were also discussed. Additionally, applications of hybrid energy systems, their benefits, drawbacks, and challenges, along with the overview of energy storage methods for renewable energy systems, were described. This study highlighted the future developments of hybrid energy systems, promising a sustainable option for power generation [16].

Sun et al. [34] analyzed two different IRESs to meet the electricity needs of a sizable office complex in Changchun. A comparison between the two was also provided to determine the best capacity of the suggested IRESs. The first and second IRES had load requirements of 5,000 kWh/d. The first IRES was made up of a solar PV, a WT, and a BB. The second IRES were made up of a solar PV system, a WT, a BB, an electrolyzer, and a hydrogen tank. Tong et al. [35] stated that solar and wind sources could supply at least 72% of the immediate demand for power without extra annual generation or energy storage in major countries if systems were configured to fulfill time-integrated annual electricity consumption and transmission restrictions were ignored. According to earlier studies, a solar and wind power system could meet 85% of the total electricity demand in the contiguous U.S. Solar and wind resources could attain higher reliability levels by introducing energy storage, boosting the installation capacity (i.e., producing power in excess of annual demand), or pooling resources from adjacent locations. Srivastava [36] suggested that the most effective use of PV-WT technology was for off-grid services, which could reach remote areas without the need for costly electrical network expansion. As a result, standalone systems powered by renewable energy sources have gained popularity. Therefore, IRES is the best option as it has significant performance and cost benefits, and can be customized to meet the needs of different end users [37].

Memon et al. [38] showed that a BB was required to store excess energy, primarily from solar panels, and to return this energy during times of deficiency to guarantee high reliability in standalone cases. The battery backup system could be abandoned if its reliability fell below 90% without sacrificing economics. The ideal hydroelectricity configuration was the least expensive energy source operating at full capacity regardless of reliability levels. They discovered that payments received by the system for the excess electric energy supply had a minor effect

on the leveled energy cost. The gain could be improved by increasing the hardware size or supply.
In 1943, neurophysiologist Warren McCulloch and mathematician Walter Pitts designed a computational model for NN. However, Ivahnenko and Lappa published the first functional multi-layered network in 1965. Artificial NN or simply NN are computational systems like the networks of biological neurons constituting the human brain. The neurons could be assumed to be processing units connected through "synaptic weights" and form the network architecture [39]. This paper used a multi-layered architecture of NN with three layers, as seen in *Figure 3*[40]. The input or the first layer received input in the problem's context. The hidden or second layer focused on updating the weights between the first and third layers. The output or third layer showed the optimization results.

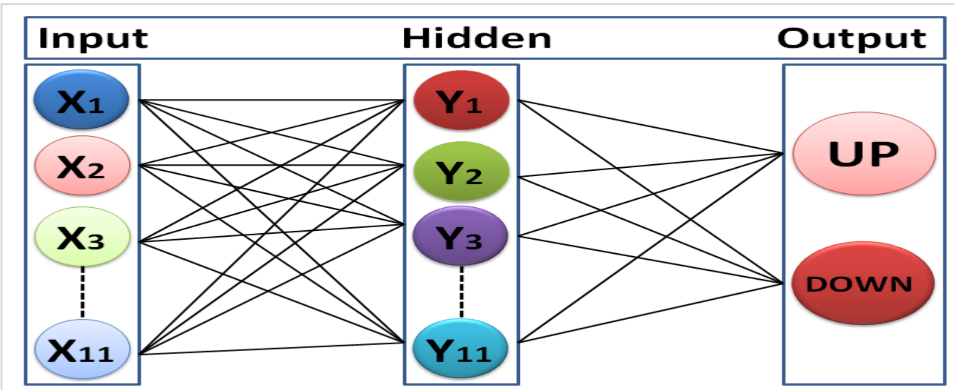

Figure 3 NN structure

Fast learning from experience and error-minimizing capabilities make NN dynamic and predictive for new outcomes. Earlier research was primarily based on classical optimization techniques with the predominant use of linear programming for simplified models and various non-linear programming methods for detailed IRES models [38]. Kumar and Palwalia [41] suggested that optimization techniques using an artificial intelligence approach could optimize global optimal power generation using off-grid IRES.

According to the literature, hybrid power systems have various combinations in practice, like fossil fuel(diesel/petrol)-battery-grid, PV-battery-grid, and hydro-PV-battery, where fossil fuel-based systems increase pollution, face source shortage, and are highly priced [42]. Hydro and thermal sources have limited availability and suitability while considering dependability on the grid. Coal-based plants experience irregular supply and shortage of coal. Hydropower plants degrade or breakdown due to natural calamities like floods, heavy rain, and landslides. Also, grid-based electric power has high prices due to input, maintenance, and transmission costs. As the grid is the primary electricity source, it faces high demand, line losses, and irregular load shading. Therefore, grid-based hybrid systems are unreliable, especially in remote areas.

These observations provided a basis for an independent power system like PV-WT-BB, enabling continuous power supply due to complementarity. This system is more reliable in remote rural areas because it is customizable according to the required load and cannot breakdown due to faults in other networks/units as it is off-grid. Its small setup has easy and low maintenance due to MPPT technology, providing optimal and regulated charging/supply [36].

This study proposed a neural architecture-based model to investigate a standalone IRES. Numerical examples, along with the original and optimized reliability, sensitivity, and profit, were provided to emphasize the findings [43]. Implementations of NN were correlated with different disciplines in the present scenario, such as pattern recognition, system optimization, and deep learning. It consisted of several methods, out of which FFBPNN was preferred to enhance the performance of the system. Although it is more flexible to modify the IRES as per the local availability of natural resources, a balance between the efficiency of units, establishment costs, and resource availability must be maintained. More accuracy is required to determine the reliability of the system and maximize its availability.

3.Method

3.1System description

For decades, the power crisis has been a global issue. However, IRESs are gaining popularity due to the advancements in the renewable energy sector. An energy-generating system is an integrated one if it consists of at least two or more renewable energy systems. The integrated systems may have several combinations of subsystems as per the localized availability of natural resources, such as solar radiation, wind velocity [44], hydropower, tide and waves, geothermal energy, and biomass[6, 7, 35]. All these sources are combined reasonably to provide a highly efficient and continuous power supply. There are two types of IRESs based on the use of grid power:

1.Standalone renewable energy systems (Off-Grid power systems)

2.Grid-connected renewable energy systems (On-Grid power systems)

It also depends on a targeted remote area, establishment cost, and environmental conditions.

This study of a standalone IRES considered a power generation system consisting of five units described as follows (*Figure 4*):

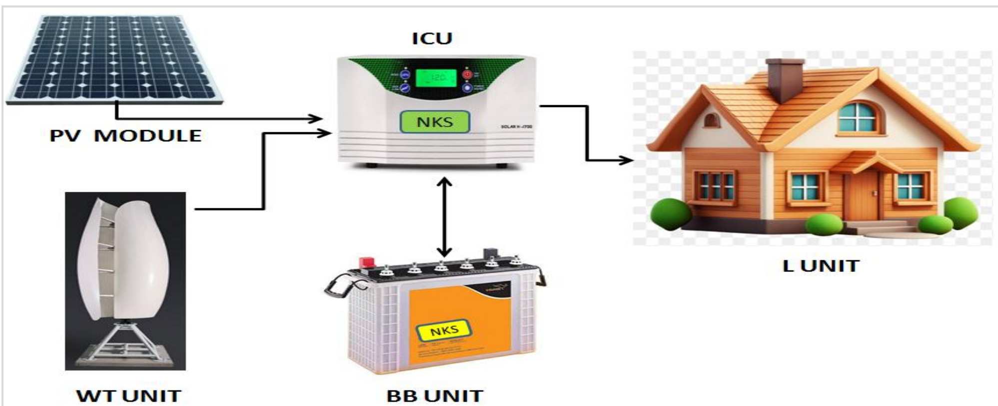

Figure 4 Block diagram of a standalone IRES

Unit1: PV module: This unit produced an electric current when exposed to solar radiation. It is generally placed facing the south direction. The solar modules have different arrangements of silicon semiconductors. These modules may be mono- or polycrystalline based on the silicon source. Monocrystalline modules are slightly more efficient but costlier than polycrystalline modules. Presently, solar modules are available to supply direct current (DC) or alternating current (AC) as per requirements. This study considered DC supply modules.

There are many reasons affecting the efficiency of the modules, decreasing their working capacity and even failing the power generation of the whole unit [45]. Some of the popular reasons are as follows:

a) Impure or low-quality manufacturing material of the PV cell.

b) Surrounding temperature of the module.

c) Bad environmental conditions, like decreased solar intensity, cloudy skies, and rain.

d) Wrong direction of sunlight exposure and setup altitude.

e) Effects of shading.

f) Wear and tear due to wind.

Unit2: WT unit: A WT, installed in wide-open windy areas, generates electric current using the wind velocity at an optimum height. WTs are of two types: horizontal-axis and vertical-axis types, with their blades rotating parallel and perpendicular to the horizon, respectively. This study considered a small vertical-axis type WT because it is more efficient and works even at slow air speeds. Its multiple units could be used as required and fixed at various places due to its size. WTs may have fixed or variable speeds according to wind availability. Generally, WT generators with fixed speeds are used to produce electricity. Some conditions leading to failed or reduced power production from a WT are as follows:

a) Wind velocity not in the range of 5 to 25 m/s.

b) Fluctuations in wind velocity.

c) Variability in the wind speed with height and areal energy distribution.

d) Disturbances due to the tower shadow effect.

Unit3: BB unit: It was a power storage facility connected to the control unit and operating in both directions. It was not connected directly to the PV and WT. It could store the surplus power when the PV and WT generate more power than the load demand. It could supply the stored power in the future when a failure occurred in Units 1 or 2 or due to a shortage of supply. BB made a major contribution to improving the system reliability. However, BB may fail or work imperfectly due to voltage fluctuations, battery temperatures, poor battery maintenance, cross-connections between terminals, shelf life, or environmental faults.

Unit4: Intelligent control unit (ICU): It is a setup of the convertor (DC/AC or AC/DC), and charges the controller systems. It was connected to the other four units of the IRES. The converter could function like an inverter or rectifier as per the charge flow direction. The ICU also consisted of devices for voltage fluctuation control, charge control, and others. It was connected to the PV and WT, and it intelligently controlled the surplus current and electric power flow to provide a seamless power supply. The ICU would fail due to a subsystem fault, voltage fluctuations, fuse blow, short-circuit, or an overload.

Unit5: L unit: It is the consumption segment of the system. It was connected to the ICU and received electrical power as per the demand profile. Generally, this unit fails due to factors like environmental failures, short-circuits, and voltage fluctuations.

This study used the transition state diagram to create the probabilistic equations of the mathematical model for an IRES. NN algorithms were used to assess several key reliability indicators (*Figure 5*). Repairs and failures caused by faulty hardware or the environment were dispersed exponentially and used as synaptic weights in neural calculations. The back propagation algorithm used in NN to update outputs was described by Anderson [45] and other authors. The weights in multiple cycles were updated using the learning course of action in the back propagation of NN to improve the results of reliability parameters. Also, a method employing the back-propagation neural network (BPNN) technique was developed to forecast reliability, profit function, and corresponding .m file code in MATLAB.

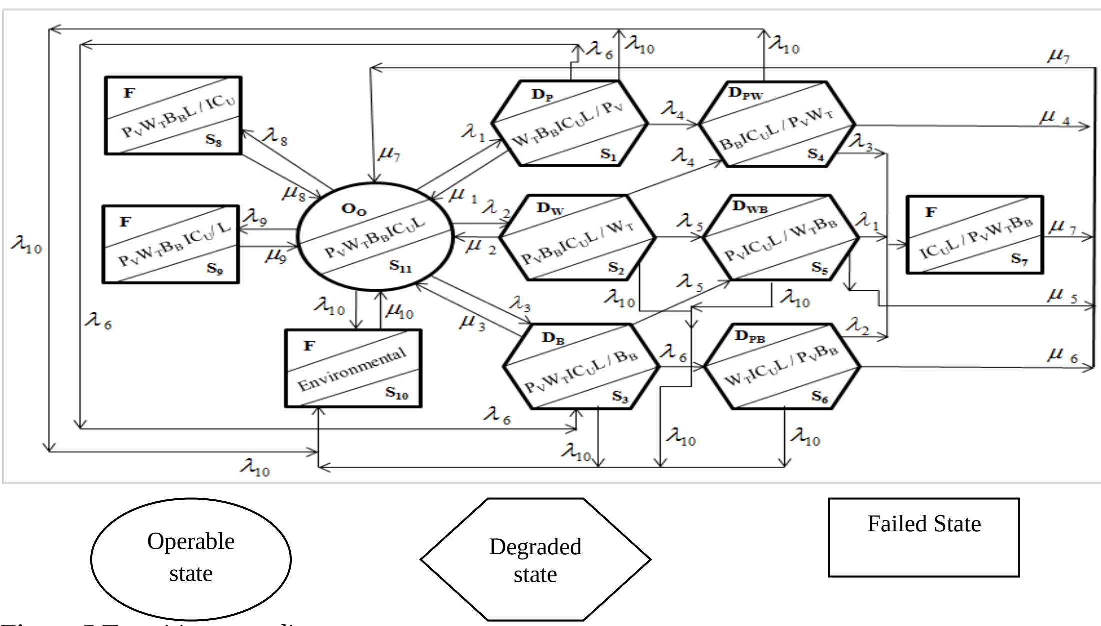

Figure 5 Transition state diagram

3.2Assumptions

3.1.1 At the start of the operation, every component/unit was in good and completely functional condition.

3.1.2 The states were statistically independent for all components involved in the operation of the system.

3.1.3 The system had five units: PV modules, WT, BB, ICU and L.

3.1.4 The system operated at lower efficiencies if any one or two of the PV/WT/BB units malfunctioned.

3.1.5 If the system was operated in a degraded state, malfunction of the power generating or battery units may breakdown or negatively affect the performance of other units.

3.1.6 The IRES may fail completely if the PV/WT/BB units or the power control unit and load failed concurrently.
3.1.7 The IRES may potentially fail due to the environmental failure.
3.1.8 The repair and failure rates of the system were distributed exponentially.
3.1.9 Synaptic weights corresponded to the failures and repairs of the system.
3.1.10 The repaired subsystem(s) would perform as if they were new.

3.3Notations

$P_i\,(t)$	i^{th} state probability at time t, $i \in \{1,2,3 \dots \dots 11\}$
$P_i\,(t+\Delta t)$	i^{th} state probability at time (t+Δt),$i \in \{1,2,3 \dots \dots 11\}$
λ_1	PV unit failure
λ_2	Failure of the WT unit
λ_3	Failure of the BB unit
λ_4	Failure of the PV+WT unit
λ_5	Failure of the WT+BB unit
λ_6	Failure of the PV+BB unit.
λ_7	Failure of the PV+WT+BB unit.
λ_8	ICU failure
λ_9	Failure of the load unit
λ_{10}	Environmental failure
λ_{11}	System breakdown
μ_1	PV unit repair
μ_2	WT unit repair
μ_3	BB unit repair
μ_4	PV+WT unit repair
μ_5	WT+BB unit repair
μ_6	PV+BB unit repair
μ_7	PV+WT+BB unit repair
μ_8	ICU repair
μ_9	Load unit repair
μ_{10}	Environmental repair
P_{up}	Probability of operable state
P_{down}	Probability of system breakdown state

3.4Development of a mathematical model

Using fundamental probability terminology, Equations 1-13 govern the behavior of the system, determining its characteristics and transition states, as follows:

$$P_1(t+\Delta t) = (1-\mu_1\Delta t-\lambda_4\Delta t-\lambda_6\Delta t-\lambda_{10}\Delta t)P_1(t)+\lambda_1 P_{11}(t)\Delta t \tag{1}$$

$$P_2(t+\Delta t) = (1-\mu_2\Delta t-\lambda_4\Delta t-\lambda_5\Delta t-\lambda_{10}\Delta t)P_2(t)+\lambda_2 P_{11}(t)\Delta t \tag{2}$$

$$P_3(t+\Delta t) = (1-\mu_3\Delta t-\lambda_5\Delta t-\lambda_6\Delta t-\lambda_{10}\Delta t)P_3(t)+\lambda_3 P_{11}(t)\Delta t \tag{3}$$

$$P_4(t+\Delta t) = (1-\mu_4\Delta t-\lambda_3\Delta t-\lambda_{10}\Delta t)P_4(t)+\lambda_4 P_1(t)\Delta t+\lambda_4 P_2(t)\Delta t \tag{4}$$

$$P_5(t+\Delta t) = (1-\mu_5\Delta t-\lambda_1\Delta t-\lambda_{10}\Delta t)P_5(t)+\lambda_5\Delta t P_2(t)+\lambda_5\Delta t P_3(t) \tag{5}$$

$$P_6(t+\Delta t) = (1-\mu_6\Delta t-\lambda_2\Delta t-\lambda_{10}\Delta t)P_6(t)+\lambda_6\Delta t P_3(t)+\lambda_6\Delta t P_1(t) \tag{6}$$

$$P_7(t+\Delta t) = (1-\mu_7\Delta t)P_7(t)+\lambda_1\Delta t P_5(t)+\lambda_2\Delta t P_6(t)+\lambda_3\Delta t P_4(t) \tag{7}$$

$$P_8(t+\Delta t) = (1-\mu_8\Delta t)P_8(t)+\lambda_8\Delta t P_{11}(t) \tag{8}$$

$$P_9(t+\Delta t) = (1-\mu_9\Delta t)P_9(t)+\lambda_9\Delta t P_{11}(t) \tag{9}$$

$$P_{10}(t+\Delta t) = (1-\mu_{10}\Delta t)P_{10}(t)+[P_1(t)+P_2(t)+P_3(t)+P_4(t)+P_5(t)+P_6(t)+P_{11}(t)]\lambda_{10}\Delta t \tag{10}$$

$$\begin{aligned}P_{11}(t+\Delta t) = (1-\lambda_1\Delta t-\lambda_2\Delta t-\lambda_3\Delta t-\lambda_8\Delta t \\ -\lambda_9\Delta t-\lambda_{10}\Delta t)P_{11}(t) \\ +[\mu_1 P_1(t)+\mu_2 P_2(t)+\mu_3 P_3(t)+\mu_4 P_4(t) \\ +\mu_5 P_5(t)+\mu_6 P_6(t) \\ +\mu_7 P_7(t)+\mu_8 P_8(t)+\mu_9 P_9(t)+\mu_{10} P_{10}(t)]\,\Delta t\end{aligned} \tag{11}$$

3.5Method and solution

The interconnected variables, layers of neural architecture, and the learning mechanism used to train the system were used to examine the complex global behavior displayed by the proposed structure. The back propagation algorithm was introduced in the 1970s to study the neural models/architectures, and out of many available learning algorithms, it is frequently used to train the FFBPNN architectures. This algorithm updated the network synaptic weights by back-propagating a gradient vector where each element was defined as the derivative of an error measure concerning a parameter. Generally, the error signals are defined by differences in actual and expected outputs from the network, mandating the inference of a set of targeted outputs for the training. Therefore, it may be claimed that back propagation is a supervised training rule. Consequently, supervised network training may be used to analyze and optimize complicated mathematical problems. *Figure 6* demonstrates the logical and step-by-step workflow of the FFBPNN algorithm.

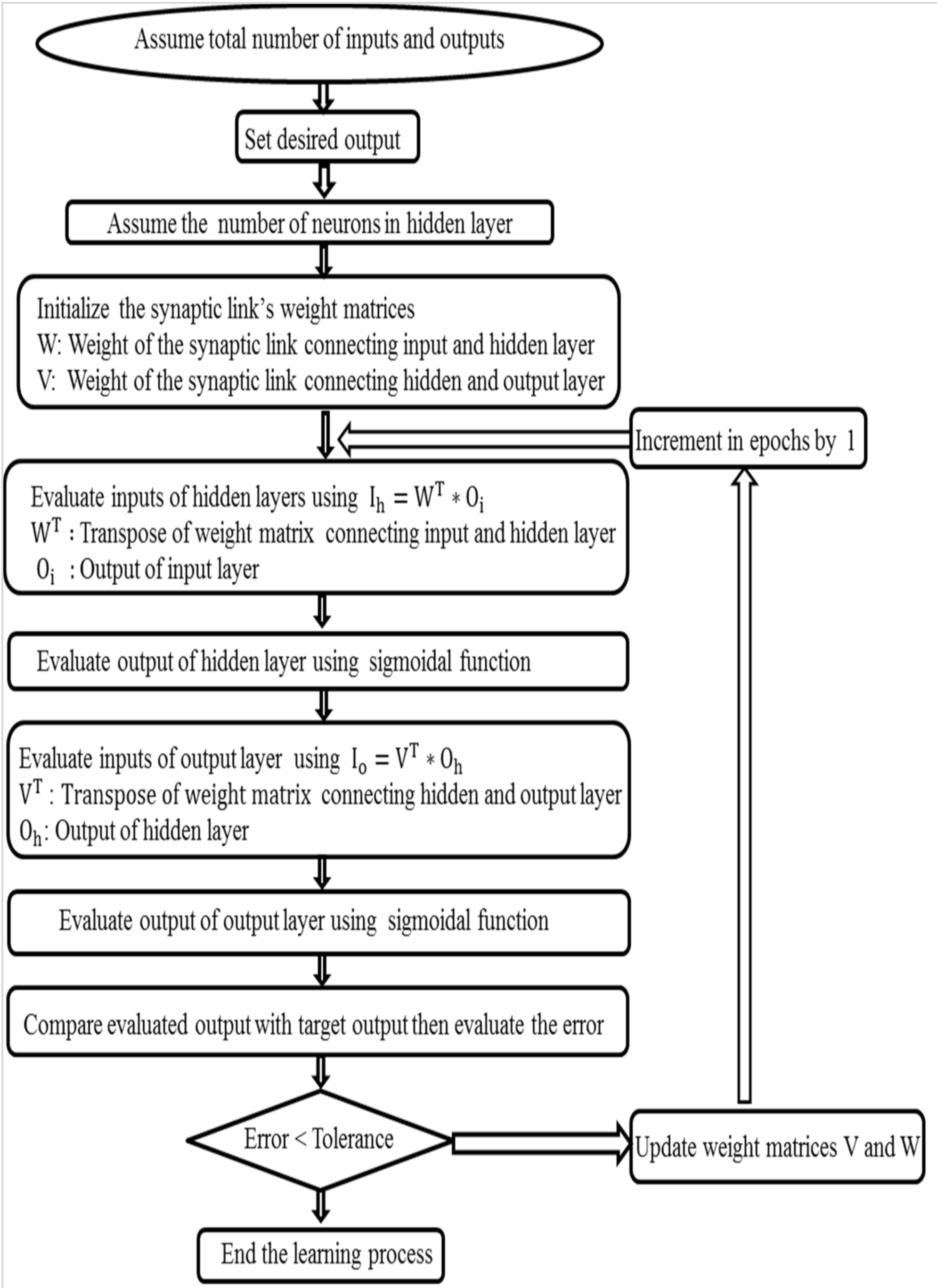

Figure 6 Workflow of the FFBPNN approach

The X_i inputs, included in the neural architecture seen in *Figure 3*, were characterized in terms of probabilities as shown in Equation 12:

$$X_i = P_i(t);\ i \in \{1,2,3 \dots \dots 11\} \qquad (12)$$

The neural outputs Y_i in the system were represented by the probabilities as shown in Equation 13:

$$Y_i = P_i(t + \Delta t);\ \ i \in \{1,2,3 \dots \dots 11\} \qquad (13)$$

The neural weight matrix governing the network set of sequences across the input and the hidden layers is as follows:

$$W = \begin{bmatrix} \phi_1 & 0 & 0 & \lambda_4\Delta t & 0 & \lambda_6\Delta t & 0 & 0 & 0 & \lambda_{10}\Delta t & \mu_1\Delta t \\ 0 & \phi_2 & 0 & \lambda_4\Delta t & \lambda_5\Delta t & 0 & 0 & 0 & 0 & \lambda_{10}\Delta t & \mu_2\Delta t \\ 0 & 0 & \phi_3 & 0 & \lambda_5\Delta t & \lambda_6\Delta t & 0 & 0 & 0 & \lambda_{10}\Delta t & \mu_3\Delta t \\ 0 & 0 & 0 & \phi_4 & 0 & 0 & \lambda_3\Delta t & 0 & 0 & \lambda_{10}\Delta t & \mu_4\Delta t \\ 0 & 0 & 0 & 0 & \phi_5 & 0 & \lambda_1\Delta t & 0 & 0 & \lambda_{10}\Delta t & \mu_5\Delta t \\ 0 & 0 & 0 & 0 & 0 & \phi_6 & \lambda_2\Delta t & 0 & 0 & \lambda_{10}\Delta t & \mu_6\Delta t \\ 0 & 0 & 0 & 0 & 0 & 0 & \phi_7 & 0 & 0 & 0 & \mu_7\Delta t \\ 0 & 0 & 0 & 0 & 0 & 0 & 0 & \phi_8 & 0 & 0 & \mu_8\Delta t \\ 0 & 0 & 0 & 0 & 0 & 0 & 0 & 0 & \phi_9 & 0 & \mu_9\Delta t \\ 0 & 0 & 0 & 0 & 0 & 0 & 0 & 0 & 0 & \phi_{10} & \mu_{10}\Delta t \\ \lambda_1\Delta t & \lambda_2\Delta t & \lambda_3\Delta t & 0 & 0 & 0 & 0 & \lambda_8\Delta t & \lambda_9\Delta t & \lambda_{10}\Delta t & \phi_{11} \end{bmatrix} \quad (14)$$

Again, the weight matrix between the output and the hidden layers is as follows:

$$V = \begin{bmatrix} w_{11} & 0 & 0 & 0 & 0 & 0 & 0 & 0 & 0 & 0 & w_{1(11)} \\ 0 & w_{22} & 0 & 0 & 0 & 0 & 0 & 0 & 0 & 0 & w_{(11)2} \\ 0 & 0 & w_{33} & 0 & 0 & 0 & 0 & 0 & 0 & 0 & w_{(11)3} \\ w_{14} & w_{24} & 0 & w_{44} & 0 & 0 & 0 & 0 & 0 & 0 & 0 \\ 0 & w_{25} & w_{35} & 0 & w_{55} & 0 & 0 & 0 & 0 & 0 & 0 \\ w_{16} & 0 & w_{36} & 0 & 0 & w_{66} & 0 & 0 & 0 & 0 & 0 \\ 0 & 0 & 0 & w_{47} & w_{57} & w_{67} & w_{77} & 0 & 0 & 0 & 0 \\ 0 & 0 & 0 & 0 & 0 & 0 & 0 & w_{88} & 0 & 0 & w_{(11)8} \\ 0 & 0 & 0 & 0 & 0 & 0 & 0 & 0 & w_{99} & 0 & w_{(11)9} \\ w_{1(10)} & w_{2(10)} & w_{3(10)} & w_{4(10)} & w_{5(10)} & w_{6(10)} & 0 & 0 & 0 & w_{(10)(10)} & w_{(11)(10)} \\ w_{1(11)} & w_{2(11)} & w_{3(11)} & w_{4(11)} & w_{5(11)} & w_{6(11)} & w_{7(11)} & w_{8(11)} & w_{9(11)} & w_{(10)(11)} & w_{(11)(11)} \end{bmatrix} \quad (15)$$

The output equations obtained using Equations 1 to 11 and weight matrices from Equations 14 and 15 are as follows:

$Y_1 = w_{11}X_1 + w_{11(1)}X_{11}$ (16)

$Y_2 = w_{22}X_2 + w_{11(2)}X_{11}$ (17)

$Y_3 = w_{33}X_3 + w_{11(3)}X_{11}$ (18)

$Y_4 = w_{44}X_4 + w_{14}X_1 + w_{24}X_2$ (19)

$Y_5 = w_{55}X_5 + w_{25}X_2 + w_{35}X_3$ (20)

$Y_6 = w_{66}X_6 + w_{16}X_1 + w_{36}X_3$ (21)

$Y_7 = w_{77}X_7 + w_{47}X_4 + w_{57}X_5 + w_{67}X_6$ (22)

$Y_8 = w_{88}X_8 + w_{11(8)}X_{11}$ (23)

$Y_9 = w_{99}X_9 + w_{11(9)}X_{11}$ (24)

$Y_{10} = w_{(10)(10)}X_{10} + w_{1(10)}X_1 + w_{2(10)}X_2 + w_{3(10)}X_3 + w_{4(10)}X_4 + w_{5(10)}X_5 + w_{6(10)}X_6 + w_{11(10)}X_{11}$ (25)

$Y_{11} = w_{(11)(11)}X_{11} + w_{1(11)}X_1 + w_{2(11)}X_2 + w_{3(11)}X_3 + w_{4(11)}X_4 + w_{5(11)}X_5 + w_{6(11)}X_6 + w_{7(11)}X_7 + w_{8(11)}X_8 + w_{9(11)}X_9 + w_{10(11)}X_{10}$ (26)

Transition states of the system could be classified as the up or down-states depending on whether they were in the operational or failure mode. The up-state and down-state probabilities of the system using Equations 16 to 26 wereas follows:

$P_{up} = Y_1 + Y_2 + Y_3 + Y_4 + Y_5 + Y_6 + Y_{11} = (w_{11}X_1 + w_{11(1)}X_{11}) + (w_{22}X_2 + w_{11(2)}X_{11}) + (w_{33}X_3 + w_{11(3)}X_{11}) + (w_{44}X_4 + w_{14}X_1 + w_{24}X_2) + (w_{55}X_5 + w_{25}X_2 + w_{35}X_3) + (w_{66}X_6 + w_{16}X_1 + w_{36}X_3) + (w_{(11)(11)}X_{11} + w_{1(11)}X_1 + w_{2(11)}X_2 + w_{3(11)}X_3 + w_{4(11)}X_4 + w_{5(11)}X_5 + w_{6(11)}X_6 + w_{7(11)}X_7 + w_{8(11)}X_8 + w_{9(11)}X_9 + w_{10(11)}X_{10})$ (27)

$P_{down}(t) = 1 - P_{up}(t)$ (28)

The reliability of the system could be stated as:

$Reliability = Y_1 + Y_2 + Y_3 + Y_4 + Y_5 + Y_6 + Y_{11}$ (29)

The profit function could be given as follows:

$G(t) = C_1 \times P_{up}(t) - C_2 \times t - C_3$ (30)

Here $C_1, C_2,$ and C_3 represent the costs of revenue, repair/ unit time, and system establishment, respectively.

$P_{up}(t)$ represents the probability for operable states.

3.6 Reliability-based sensitivity analysis

The sensitivity of the system with respect to the failure of PV (λ_1), WT (λ_2), BB (λ_3), and environmental failure (λ_{10}) could be evaluated in terms of reliability. The relevant equations are as follows:

$$\frac{\partial P_{up}}{\partial \lambda_1} = -P_5(t)\Delta t \quad (31)$$

$$\frac{\partial P_{up}}{\partial \lambda_2} = -P_6(t)\Delta t \quad (32)$$

$$\frac{\partial P_{up}}{\partial \lambda_3} = -P_4(t)\Delta t \quad (33)$$

$$\frac{\partial P_{up}}{\partial \lambda_{10}} = -[P_1(t) + P_2(t) + P_3(t) + P_4(t) + P_5(t) + P_6(t) + P_{11}(t)]\Delta t \quad (34)$$

4. Results

This study had the following assumptions to examine the outcomes of the system under consideration:

$\mu_i = 1, \quad i \in \{1,2,3 \dots 10\}; \quad \lambda_1 = 0.02,$
$\lambda_2 = 0.02, \quad \lambda_3 = 0.025,$
$\lambda_4 = 0.01,$
$\lambda_5 = 0.01,\ \lambda_6 = 0.01,\ \lambda_8 = 0.01,\ \lambda_9 = 0.001,$
$\lambda_{10} = 0.01,$

Equations 28 and 29 provided unreliability and reliability, respectively. Their results are displayed in *Figures 7* and *8* and are given in *Table 1*. Observing *Table 1* and *Figure 7*, the reliability increased significantly in the first 100 iterations and then slowly till 624 iterations. At the last cycle reliability $P_{up}(t)$ reached .99 which is precise up to 0.0001. Also, from *Figure 8* and *Table 1*, unreliability $P_{down}(t)$ decreased catastrophically in initial iterations and then slowly afterward. These results show that the system is highly reliable in early life and becomes stable during useful life.

Equation 30 is used to compute the profit values. For the study and comparison of the profit values, the installation cost $C_3 = 100$ units, revenue cost $C_1 = 80$ units, and variable repair costs $C_2 = 20, 50, 70,$ and 80 units. *Figure 9* and *Table 2* illustrate the profit function values derived from Equation 30. It is evident that the system remains profitable until the repair costs C_2 reach 20, 50, and 70 units. However, it is advisable to replace major components with new ones, as significant revenue losses become apparent when the repair cost C_2 exceeds 70 units.

4.1 Sensitivity analysis

During investigations, it is observed that the claimed life of the PV module, WT is longer in comparison with the life span of batteries in BB. Therefore, BB may attract more failures in a certain duration which implies that the system is more sensitive to BB in comparison with WT and PV modules. As represented visually in *Figure 10* and statistically in *Table 3*, the data obtained from Equations 31-34 was investigated to examine the sensitivity of the system corresponding to different failures. While it is minimum, moderate, and highly sensitive to failures in PV module, WT, and BB respectively. The graphs have shown that the system may face breakdowns under environmental failure during its whole early and useful life.

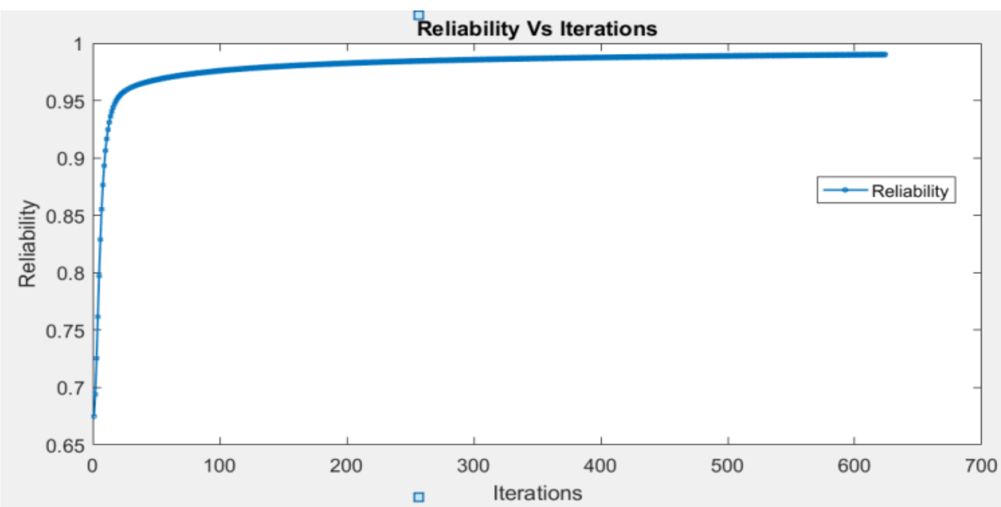

Figure 7 Reliability vs. Iterations

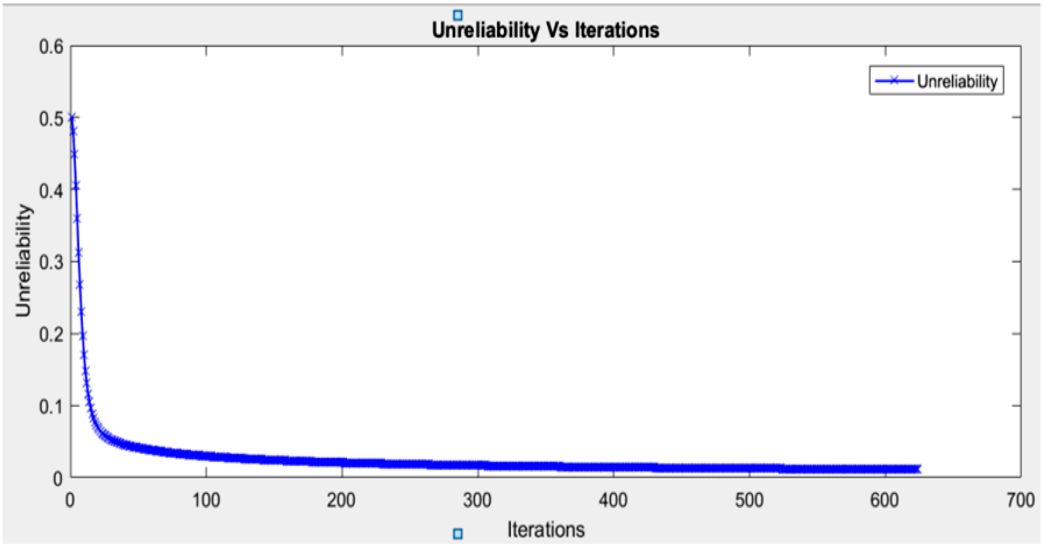

Figure 8 Unreliability vs. Iterations

Table 1 Reliability vs. Iterations

Iterations	**1**	**25**	**50**	**100**	**150**	**200**	**250**
$P_{up}(t)$	0.6749	0.9581	0.9681	0.9759	0.9799	0.9824	0.9842
$P_{down}(t)$	0.3251	0.0419	0.0319	0.0241	0.0201	0.0176	0.0158
ITERATIONS	300	350	400	450	500	550	624
$P_{up}(t)$	0.9856	0.9866	0.9875	0.9882	0.9888	0.9892	0.990
$P_{down}(t)$	0.0144	0.0134	0.0125	0.0118	0.0112	0.0106	0.010

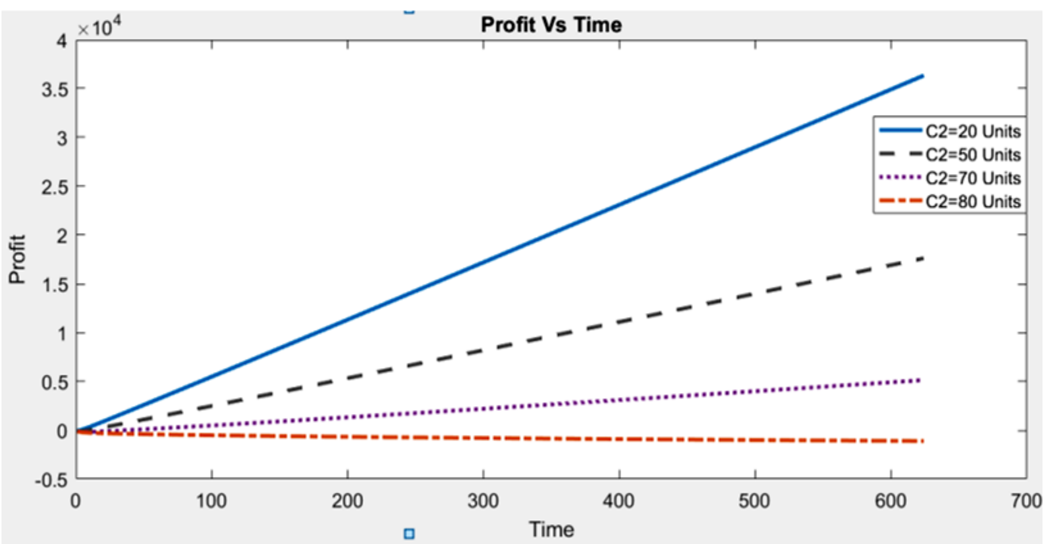

Figure 9 Comparison between profit and time

Table 2 Values of profit function for diverse repair cost over time/epochs

	Profit (values of C_2 in units)			
Time/ Epochs	**80**	**70**	**50**	**20**
1	-126.006921	-116.006921	-96.006921	-66.006921
25	-325.140773	-75.140773	424.859227	1174.85923
50	-396.678434	103.321566	1103.32157	2603.32157

Time/ Epochs	Profit (values of C_2 in units) 80	70	50	20
100	-506.24321	493.75679	2493.75679	5493.75679
150	-593.724443	906.275557	3906.27556	8406.27556
200	-668.584393	1331.41561	5331.41561	11331.4156
250	-734.995774	1765.00423	6765.00423	14265.0042
300	-795.242926	2204.75707	8204.75707	17204.7571
350	-850.738035	2649.26197	9649.26197	20149.2620
400	-902.42628	3097.57372	11097.5737	23097.5737
450	-950.976956	3549.02304	12549.0230	26049.0230
500	-996.884441	4003.11556	14003.1156	29003.1156
550	-1040.52612	4459.47388	15459.4739	31959.4739
600	-1082.19776	4917.80224	16917.8022	34917.8022
624	-1101.57176	5138.42824	17618.4282	36338.4282

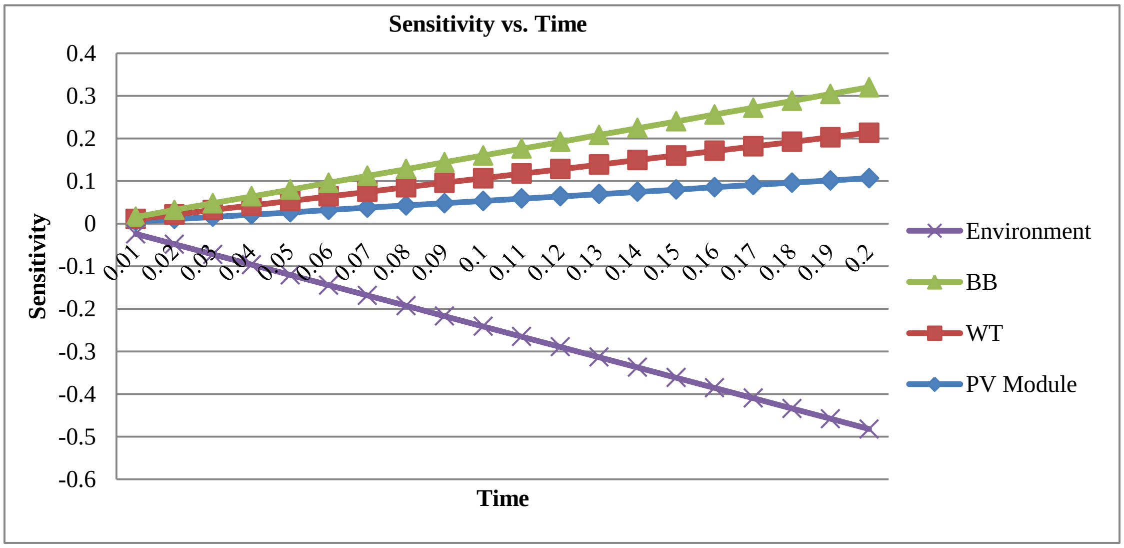

Figure 10 Sensitivity vs. Time

Table 3 Sensitivity vs. Time

Δt	$\frac{\partial P_{up}}{\partial \lambda_1}$	$\frac{\partial P_{up}}{\partial \lambda_2}$	$\frac{\partial P_{up}}{\partial \lambda_3}$	$\frac{\partial P_{up}}{\partial \lambda_{10}}$
0.01	0.00534	0.00534	0.005341	-0.040135
0.02	0.01068	0.01068	0.010682	-0.08027
0.03	0.01602	0.01602	0.016023	-0.120405
0.04	0.02136	0.02136	0.021364	-0.16054
0.05	0.0267	0.0267	0.026705	-0.200675
0.06	0.03204	0.03204	0.032046	-0.24081
0.07	0.03738	0.03738	0.037387	-0.280945
0.08	0.04272	0.04272	0.042728	-0.32108
0.09	0.04806	0.04806	0.048069	-0.361215
0.1	0.0534	0.0534	0.05341	-0.40135
0.11	0.05874	0.05874	0.058751	-0.441485
0.12	0.06408	0.06408	0.064092	-0.48162
0.13	0.06942	0.06942	0.069433	-0.521755
0.14	0.07476	0.07476	0.074774	-0.56189
0.15	0.0801	0.0801	0.080115	-0.602025
0.16	0.08544	0.08544	0.085456	-0.64216
0.17	0.09078	0.09078	0.090797	-0.682295

Δt	$\frac{\partial P_{up}}{\partial \lambda_1}$	$\frac{\partial P_{up}}{\partial \lambda_2}$	$\frac{\partial P_{up}}{\partial \lambda_3}$	$\frac{\partial P_{up}}{\partial \lambda_{10}}$
0.18	0.09612	0.09612	0.096138	-0.72243
0.19	0.10146	0.10146	0.101479	-0.762565
0.2	0.1068	0.1068	0.10682	-0.8027

5.Discussion

The preliminary reliability of the system was 0.6749, according to *Table 1*. After a significant number of iterations or epochs, the gradient descent method of back propagation was employed in NN to update the weights of synapses that were used as failures or repairs. The reliability of the system reached a maximum of 0.99 in 624 iterations with an acceptable range of 10^{-4}. The corresponding unreliability values are also shown in *Table 1*. The reliability and unreliability values are depicted in *Figures 7* and *8*, respectively. The reliability of the system was improved iteratively, signifying the BPNN concept, specifically in complicated engineering systems.

The profit function steadily increased with the iterations, as shown from the outputs of Equation 30 and the data represented in *Table 2*. The comparison between profit and various repair costs is depicted in *Figure 9*. As depicted in *Table 2*, the profit function in each cycle had the maximum value for smaller repair costs, i.e., 20 units and when repair cost crosses 70 unit then it is an indication for major component replacement to improve the performance as good as new system. It can stimulate the decision-making of the system managers. A reasonable repair cost is a good option to maintain the system because the replacement costs for new components are a challenge in renewable power generation systems. Though continued research has decreased the prices, necessary components are still costly. To compare Mono and polycrystalline PV Modules, vertical and horizontal axis WT *Table 4* and *5* are given below:

Table 4 Comparison between PV modules

	Cost	Efficiency	Advantage	Heat resistance
Monocrystalline PV	Expensive	High	Efficient and space saver	High
Polycrystalline PV	Affordable	Less	Medium cost and efficiency	Low

Table 5 Comparison between WT with vertical and horizontal axes

	Installation Cost	Efficiency	Maintenance cost	Space required	Wind speed	Advantage
WT with vertical axis	Low	Low/Medium	Low	Rooftop	Moderate to low	Small size and components
WT with horizontal axis	High	High	High	Large and open	High	Massive structure

The sensitivity of the system to the failures for the PV(λ_1), WT(λ_2), BB(λ_3), and the environment (λ_{10}) are shown in *Table 3*. When the system was exposed to various environmental obstacles during operation, like temperature, dust, clouds, and humidity, its performance/efficiency is hampered. The nature of sensitivity depicted in *Figure 10* easily indicated that a standalone IRES was more sensitive to environmental failure, signifying the importance of the environmental conditions under which the proposed IRES was operated.

As shown in *Table 4* and *Figure 11*, the data collected for mono and polycrystalline PV modules of 100 Watts for 15 days recommended monocrystalline PV modules over ordinary polycrystalline PV modules. The monocrystalline PV modules were more efficient than the polycrystalline ones [46–48]. The rotor power coefficient (C_P) with respect to tip-speed ratio is slightly smaller for vertical axis WT (Darrieus rotor type) which makes it suitable for proposed model of standalone IRES.

As illustrated in *Table 5* and *Figure 12*, the power coefficient (C_P) for vertical-axis wind turbines (Darrieus type) ranges from 0.3 to 0.4 with respect to a tip speed ratio of 4 to 6. In contrast, 2 and 3-bladed horizontal-axis wind turbines require a higher tip speed ratio to achieve a slightly increased rotor C_P.

Therefore, the less efficient small or medium-sized vertical-axis WT (Darrious type) were recommended over the more efficient large horizontal-axis WT because the advantages that they had low maintenance, worked even in slow air velocities, were wind-direction independent, saved space, and required no yaw mechanism [49, 50]. Therefore, it was obvious that the proposed system was more reliable and eco-friendlier in overall performance and behavior than other off-grid combinations of hybrid renewable power generation systems.

5.1Limitations

This study is a mathematical overview of small-scale IRES in terms of reliability that can be expanded to examine further elements of its techno-economic study. It did not take into account the variation in electricity prices with the time of day because India currently does not use such a pricing structure. It may be necessary to impose time-dependent prices due to the increasing share of renewable energy sources.

A complete list of abbreviations is shown in *Appendix I*.

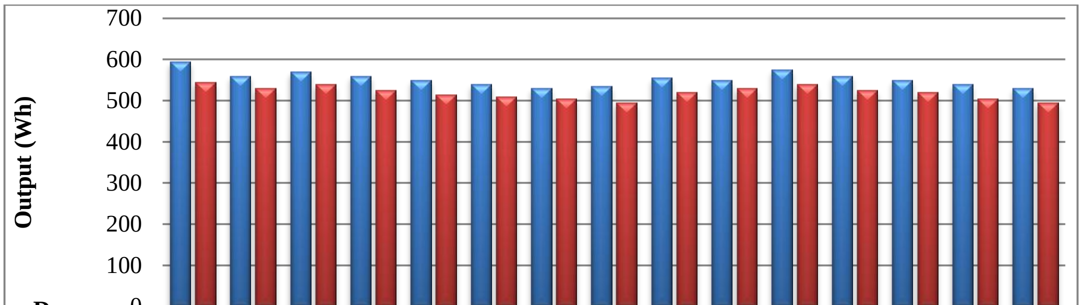

Days	1	2	3	4	5	6	7	8	9	10	11	12	13	14	15
Mono PV	595	560	570	560	550	540	530	535	555	550	575	560	550	540	530
Poly PV	545	530	540	525	515	510	505	495	520	530	540	525	520	505	495

Figure 11 Power production performance

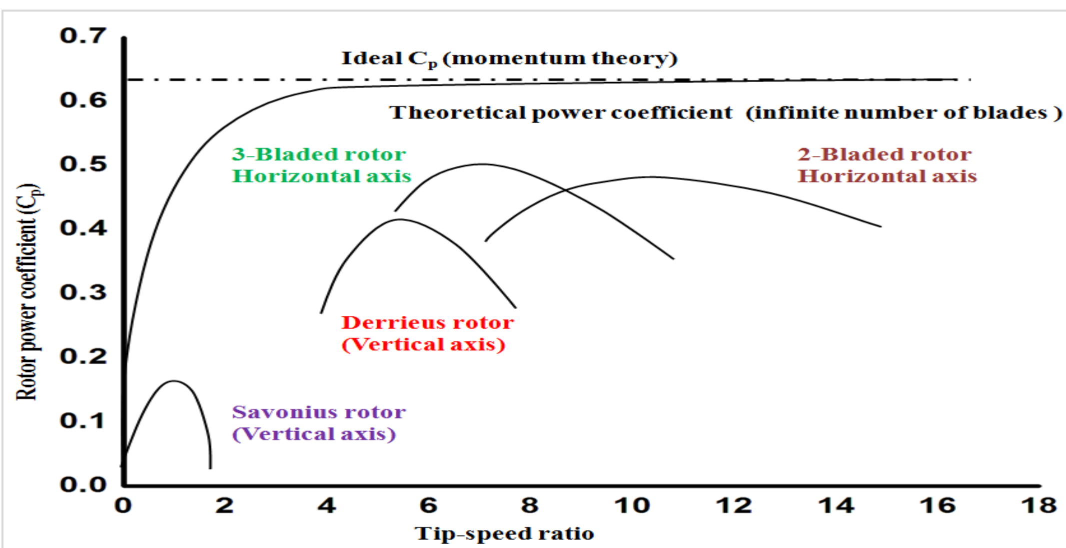

Figure 12 Comparison of the efficiency of WT with vertical and horizontal axes

6.Conclusion and future work

This paper investigated the reliability, cost, and sensitivity of a standalone IRES featuring monocrystalline PV, efficient vertical-axis WT, and solar-compatible BB. The system proves reliable in remote areas lacking grid connectivity, with ample wind and solar resources. Connected to BB for backup during low production or electricity shortages, it minimizes breakdowns. While initial costs are high, ongoing research reduces expenses, and low maintenance, coupled with a recovery period, adds value. The system exhibits low sensitivity to BB and high sensitivity to environmental conditions, addressable with advanced components and AI-driven fault prediction. Scaling PV modules, WT units, and BBs can enhance production and environmental benefits, fostering a reliable, eco-friendly future. This study advocates harnessing local natural resources to meet future demands for green electrical energy. Customizable vertical-axis WT can optimize power recovery in low wind speed areas, particularly in North India. The authors plan to hybridize WT with scaled solar PV systems for field testing and certification. The analysis and creation of wind/PV system models for small-scale power generation will be crucial for future studies. These findings provide a viable solution to energy challenges at local and global scales, encouraging key players to integrate PV and wind systems in remote locations. The proposed IRES concept could extend to meet high electric power demands for EV charging stations and battery-swapping centers on highways, expressways, and remote routes. Further studies are essential to reduce operational costs, enhance maintenance, and develop efficient power banks and optimized control/conversion units for the renewable energy industry. A balanced prediction of load demand and supply management is crucial for establishing and operating an IRES. A standalone IRES with PV-WT-BB emerges as a practical solution to fulfil electric power demands in remote areas, contributing significantly to sustainable and reliable electrification and overcoming the electrical energy crisis.

Acknowledgment
None.

Conflicts of interest
The authors have no conflicts of interest to declare.

Data availability
Not applicable.

Author's contribution statement
Nitin Kumar Sharma: Conceptualization, methodology, validation, formal analysis, investigation, data curation, and writing- original draft, review, and editing. **Dr. Sachin Kumar:** Analytical review, validation, and formal analysis of inputs of all co-authors. **Dr. Pradeep Kumar Yadav:** Review and formal analysis. **Dr. Ekata:** Conceptualization, methodology, software, and validation.

References
[1] Khosravani A, Safaei E, Reynolds M, Kelly KE, Powell KM. Challenges of reaching high renewable fractions in hybrid renewable energy systems. Energy Reports. 2023; 9:1000-17.

[2] Das U, Mandal S, Bhattacharjee S, Nandi C. A review of different configuration of hybrid energy systems with case study analysis. International Journal of Environment and Sustainable Development. 2022; 21(1-2):116-37.

[3] Javeed I, Khezri R, Mahmoudi A, Yazdani A, Shafiullah GM. Optimal sizing of rooftop PV and battery storage for grid-connected houses considering flat and time-of-use electricity rates. Energies. 2021; 14(12):1-19.

[4] Farhat O, Khaled M, Faraj J, Hachem F, Taher R, Castelain C. A short recent review on hybrid energy systems: critical analysis and recommendations. Energy Reports. 2022; 8:792-802.

[5] Johannsen RM, Østergaard PA, Hanlin R. Hybrid photovoltaic and wind mini-grids in Kenya: techno-economic assessment and barriers to diffusion. Energy for Sustainable Development. 2020; 54:111-26.

[6] Amuta EO, Wara ST, Agbetuyi AF, Adoghe UA, Olajube A. Reliability assessment of an off-grid hybrid micro-grid power system (HMPS) for a remote community in Nigeria. In IOP conference series: earth and environmental science 2021 (pp. 1-12). IOP Publishing.

[7] Esan AB, Agbetuyi AF, Oghorada O, Ogbeide K, Awelewa AA, Afolabi AE. Reliability assessments of an islanded hybrid PV-diesel-battery system for a typical rural community in Nigeria. Heliyon. 2019; 5(5):1-13.

[8] Buscheck TA, Upadhye RS. Hybrid-energy approach enabled by heat storage and oxy-combustion to generate electricity with near-zero or negative CO_2 emissions. Energy Conversion and Management. 2021; 244:114496.

[9] Jurasz J, Beluco A, Canales FA. The impact of complementarity on power supply reliability of small scale hybrid energy systems. Energy. 2018; 161:737-43.

[10] Muchiri K, Kamau JN, Wekesa DW, Saoke CO, Mutuku JN, Gathua JK. Wind and solar resource complementarity and its viability in wind/PV hybrid energy systems in Machakos, Kenya. Scientific African. 2023; 20: e01599.

[11] Li XY, Huang HZ, Li YF. Reliability analysis of phased mission system with non-exponential and partially repairable components. Reliability Engineering & System Safety. 2018; 175:119-27.

[12] Sachin K, Anand T. Evaluation of some reliability parameters of a three state repairable system with environmental failure. International Journal of Research and Reviews in Applied Sciences. 2009; 2(1):96-103.

[13] Pradhan N, Karki NR. Probabilistic reliability evaluation of off-grid small hybrid solar PV-wind power system for the rural electrification in Nepal. In North American power symposium 2012 (pp. 1-6). IEEE.

[14] Goel S, Sharma R. Performance evaluation of stand alone, grid connected and hybrid renewable energy systems for rural application: a comparative review. Renewable and Sustainable Energy Reviews. 2017; 78:1378-89.

[15] Negi S, Mathew L. Hybrid renewable energy system: a review. International Journal of Electronic and Electrical Engineering. 2014; 7(5):535-42.

[16] Ibrahim M, Khair A, Ansari S. A review of hybrid renewable energy systems for electric power generation. International Journal of Engineering Research and Applications. 2015; 5(8):42-8.
[17] Liu H, Wu B, Maleki A, Pourfayaz F, Ghasempour R. Effects of reliability index on optimal configuration of hybrid solar/battery energy system by optimization approach: a case study. International Journal of Photoenergy. 2021; 2021:1-11.
[18] El-houari H, Allouhi A, Salameh T, Kousksou T, Jamil A, El AB. Energy, economic, environment (3E) analysis of WT-PV-battery autonomous hybrid power plants in climatically varying regions. Sustainable Energy Technologies and Assessments. 2021; 43:100961.
[19] Lakshmanan I, Ramasamy S. An artificial neural-network approach to software reliability growth modeling. Procedia Computer Science. 2015; 57:695-702.
[20] Narula K, Nagai Y, Pachauri S. The role of decentralized distributed generation in achieving universal rural electrification in South Asia by 2030. Energy Policy. 2012; 47:345-57.
[21] Patel AM, Singal SK. Economic analysis of integrated renewable energy system for electrification of remote rural area having scattered population. International Journal of Renewable Energy Research. 2018; 8(1):258-65.
[22] Ram M, Singh SB, Singh VV. Stochastic analysis of a standby system with waiting repair strategy. IEEE Transactions on Systems, Man, and Cybernetics: Systems. 2013; 43(3):698-707.
[23] Rajasekaran S, Pai GV. Neural networks, fuzzy logic and genetic algorithm: synthesis and applications (with CD). PHI Learning Pvt. Ltd.; 2003.
[24] Ishani E, Shruti J, Vijetha J, Puja N, Pooja S. Hybrid Energy System. International Journal of Engineering Research & Technology. 2017; 5(1):1-6.
[25] Roy P, He J, Zhao T, Singh YV. Recent advances of wind-solar hybrid renewable energy systems for power generation: a review. IEEE Open Journal of the Industrial Electronics Society. 2022; 3:81-104.
[26] Kumar S, Saket RK, Dheer DK, Holm-nielsen JB, Sanjeevikumar P. Reliability enhancement of electrical power system including impacts of renewable energy sources: a comprehensive review. IET Generation, Transmission & Distribution. 2020; 14(10):1799-815.
[27] Mahmoud FS, Diab AA, Ali ZM, El-sayed AH, Alquthami T, Ahmed M, et al. Optimal sizing of smart hybrid renewable energy system using different optimization algorithms. Energy Reports. 2022; 8:4935-56.
[28] Kallio S, Siroux M. Hybrid renewable energy systems based on micro-cogeneration. Energy Reports. 2022; 8:762-9.
[29] Jha N, Prashar D, Rashid M, Khanam Z, Nagpal A, Alghamdi AS, et al. Energy-efficient hybrid power system model based on solar and wind energy for integrated grids. Mathematical Problems in Engineering. 2022; 2022:1-12.
[30] Sari A, Majdi A, Opulencia MJ, Timoshin A, Huy DT, Trung ND, et al. New optimized configuration for a hybrid PV/diesel/battery system based on coyote optimization algorithm: a case study for Hotan county. Energy Reports. 2022; 8:15480-92.
[31] Khare V, Nema S, Baredar P. Reliability analysis of hybrid renewable energy system by fault tree analysis. Energy & Environment. 2019; 30(3):542-55.
[32] Ghania SM, Mahmoud KR, Hashmi AM. A reliability study of renewable energy resources and their integration with utility grids. Engineering, Technology & Applied Science Research. 2022; 12(5):9078-86.
[33] Hellel EK, Hamaci S, Ziani R. Modelling and reliability analysis of multi-source renewable energy systems using deterministic and stochastic Petri net. The Open Automation and Control Systems Journal. 2018; 10(1):25-40.
[34] Sun W, Tian C, Jin Y. Cost and reliability analysis of a hybrid renewable energy systems-a case study on an administration building. MIST International Journal of Science and Technology. 2022; 10:29-35.
[35] Tong D, Farnham DJ, Duan L, Zhang Q, Lewis NS, Caldeira K, et al. Geophysical constraints on the reliability of solar and wind power worldwide. Nature Communications. 2021; 12(1):1-12.
[36] Srivastava S. Generation of hybrid energy system (solar-wind) supported with battery energy storage. International Journal for Research in Applied Science & Engineering Technology. 2022; 10(9):1439-46.
[37] Koraki D, Strunz K. Wind and solar power integration in electricity markets and distribution networks through service-centric virtual power plants. IEEE Transactions on Power Systems. 2017; 33(1):473-85.
[38] Memon SA, Upadhyay DS, Patel RN. Optimization of solar and battery-based hybrid renewable energy system augmented with bioenergy and hydro energy-based dispatchable source. Iscience. 2023; 26(1):1-19.
[39] Pratihar DK. Soft computing: fundamentals and applications. Alpha Science International, Ltd; 2013.
[40] Patel D, Bielecki D, Rai R, Dargush G. Improving connectivity and accelerating multiscale topology optimization using deep neural network techniques. Structural and Multidisciplinary Optimization. 2022; 65(4):126.
[41] Kumar P, Palwalia DK. Decentralized autonomous hybrid renewable power generation. Journal of Renewable Energy. 2015; 2015:1-15.
[42] Basnet S, Deschinkel K, Le ML, Péra MC. A review on recent standalone and grid integrated hybrid renewable energy systems: system optimization and energy management strategies. Renewable Energy Focus. 2023.
[43] León GJC, De LASE, Aguayo AJ. A review of hybrid renewable energy systems: architectures, battery systems, and optimization techniques. Engineer. 2023; 4(2):1446-67.
[44] Ding Z, Hou H, Yu G, Hu E, Duan L, Zhao J. Performance analysis of a wind-solar hybrid power

generation system. Energy Conversion and Management. 2019; 181:223-34.
[45] Anderson JA. An introduction to neural networks. MIT press; 1995.
[46] https://www.solarsquare.in/blog/types-of-solar-panels/. Accessed 12 November 2023.
[47] Mirzaei M, Mohiabadi MZ. A comparative analysis of long-term field test of monocrystalline and polycrystalline PV power generation in semi-arid climate conditions. Energy for Sustainable Development. 2017; 38:93-101.
[48] Taşçıoğlu A, Taşkın O, Vardar A. A power case study for monocrystalline and polycrystalline solar panels in Bursa City, Turkey. International Journal of Photoenergy. 2016; 2016:1-8.
[49] Kamran M. Fundamentals of Smart Grid Systems. Elsevier; 2022
[50] Muratoğlu A, Demir MS. Numerical analyses of a straight bladed vertical axis darrieus wind turbine: verification of DMS algorithm and Qblade code. European Journal of Technique. 2019; 9(2):195-208.

Nitin Kumar Sharma is an Assistant Professor at Ajay Kumar Garg Engineering College, Ghaziabad, and a research scholar at the KIET Group of Institutions, Ghaziabad, Delhi-NCR, India affiliated with AKTU, Lucknow. He earned his M.Sc. in Mathematics from CCS University, Meerut, India, and his M.Phil. from the School of Basic and Applied Sciences at Shobhit University, Meerut, India. He has contributed to the field with four research papers published in international peer-reviewed journals. His research interests lie in the areas of Reliability and Operations research.
Email: nitmaths@yahoo.co.in

Dr. Sachin Kumar is a Professor at the KIET Group of Institutions, located on the Meerut Road (NH-58) in Delhi-NCR, Ghaziabad, India. He earned his Ph.D. in Mathematics from CCS University, Meerut, India. Dr. Kumar's academic contributions include two patents and 19 research papers published in peer-reviewed international journals. He is also the author of a book on engineering mathematics. Currently, he is supervising three Ph.D. scholars. In addition to his teaching and research roles, Dr. Kumar is an active member of the editorial boards of various international journals and holds life memberships in IAENG and ISTE, New Delhi, India. His research interests are focused on Reliability and Operations research.
Email:sachin.kumar@kiet.edu

Dr. Pradeep Kumar Yadav holds the positions of Professor and Principal Technical Officer at the Central Building Research Institute, Roorkee, Uttarakhand, India. He earned his Ph.D. in Mathematics from Gurukul Kangri Vishwavidyalaya, Haridwar, Uttarakhand, India. Dr. Yadav has made significant academic contributions, having published 146 research papers in peer-reviewed international journals. He has successfully supervised four research scholars and is currently overseeing the work of two additional scholars. His research interests include distributed systems, mathematical modeling, and operations research.
Email: prd_yadav@rediffmail.com

Dr. Ekata is a Professor at the KIET Group of Institutions in Delhi-NCR, situated on Meerut Road (NH-58), Ghaziabad, India. She holds a Ph.D. in Mathematics and a Master's degree in Computer Application, both from CCS University, Meerut, Uttar Pradesh, India. Dr. Ekata has published 24 research papers in peer-reviewed international journals and co-authored two books on applied mathematics. She is actively involved as a reviewer and a member of the editorial boards of various international journals. Additionally, she is a life member of ISTE, New Delhi, India. Her research interests encompass reliability, operations research, and soft computing.
Email: ekata@kiet.edu

Appendix I

S. No.	Abbreviation	Description
1	AC	Alternating Current
2	BB	Battery Bank
3	BPNN	Back-Propagation Neural Network
4	C_p	The Rotor Power Coefficient
5	DC	Direct Current
6	EV	Electric Vehicle
7	FFBPNN	Feed Forward Back Propagation Neural Network
8	HRES	Hybrid Renewable Energy Systems
9	ICU	Intelligent Control Unit
10	IRES	Integrated Renewable Energy System
11	L	Load
12	MPPT	Maximum Power Point Tracking
13	NN	Neural Networks
14	PV	Photovoltaic
15	TLCC	Total Lifecycle Cost
16	WT	Wind Turbine